Robotically Assisted Percutaneous Local Therapy and Biopsy
(Preliminary Investigation)

[1]Gabor Fichtinger, [2]Ken Masamune, [1,3]Alexandru Patriciu, [1]Attila Tanacs, [4]James H. Anderson, [5,3]Theodore L. DeWeese, [1]Russell H. Taylor, [3]Dan Stoianovici

[1,] Engineering Research Center, Johns Hopkins University, Baltimore

[2] Graduate School of Engineering, The University of Tokyo, Japan

[3] Brady Urological Institute, Johns Hopkins University, Baltimore

[4] Department of Radiology, Johns Hopkins University, Baltimore

[5] Department of Radiation Oncology , Johns Hopkins University, Baltimore

(Contact: Gabor Fichtinger at gabor@cs.jhu.edu)

Keywords: image-guided surgery, percutaneous needle placement, surgical robotics

Abstract We present the concept and prototype of an image-guided robotic system for accurate and consistent placement of percutaneous needles in soft tissue targets under CT-guidance. The system is a promising embodiment of the Surgical CAD/CAM paradigm and as such, easily adaptable to other image guidance modalities, like X-ray fluoroscopy. We also report the first results of pre-clinical experiments on phantoms.

1 Motivation

Our vision is that by extending human surgeons' ability to plan and carry out surgical interventions more accurately and less invasively, Computer Integrated Surgery (CIS) systems will address a vital need to greatly reduce costs, improve clinical outcomes, and improve the efficiency of health care delivery. Further, the combination of consistent execution, patient and task models, and logging of intraoperative and outcome data made possible by CIS systems will produce the same impact on surgery that has been realized in industrial CAD/CAM systems. Surgical CAD/CAM systems (Figure 1) transform preoperative images and other information to the actual patient in the operating room, assist clinicians in developing an optimized interventional plan, register this preoperative data to the actual patient in the operating, and then use a variety of appropriate means, such as robots and image overlay displays, to assist in the accurate execution of the

planned interventions. Surgical CAD/CAM systems are analogous to manufacturing CAD/CAM systems. There are three key concepts:

Figure 1: Information flow in surgical CAD/CAM systems

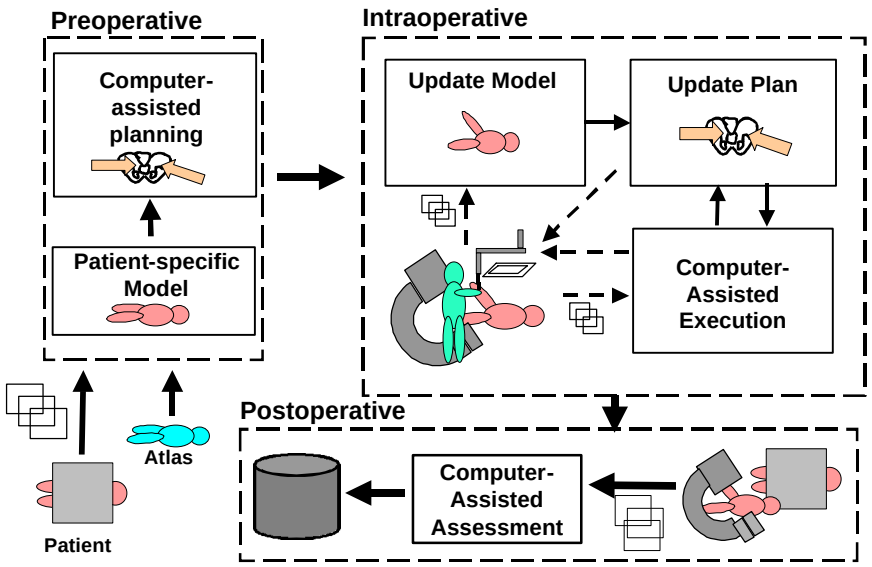

"Surgical CAD" is analogous to computer-aided design in manufacturing systems. Preoperatively, medical images, anatomical atlases, and other information are combined to make a model of an individual patient. The computer then assists the surgeon in planning and optimizing an appropriate intervention.

"Surgical CAM" is analogous to computer-aided manufacturing, with modifications to fit the specific requirements of surgery. The data from the preoperative planning step (images, models, plan geometry, etc.) is all brought into the operating room. Real time images and other sensor data are used to "register" the preoperative plan to the actual patient, and the model and the plan are updated throughout the procedure. The actual surgical procedure is performed by the surgeon with the assistance of the computer, using appropriate technology for the particular intervention.

"Surgical TQM" is analogous to "total quality management" in manufacturing, and reflects the important role that the computer can play in reducing surgical errors and in promoting more consistent and improved outcomes. It is built into the entire process.

Percutaneous therapy, which is inserting thin tubular devices (needles, cannulas, electrodes, sensory or tissue ablation probes, etc.) into the body through the skin, fits

naturally within our broader paradigm of Surgical CAD/CAM systems. The basic process involves planning a patient-specific therapy pattern, delivering the therapy through a series of percutaneous access steps, assessing what was actually done, and using this feedback to control the therapy procedure. Our goal is to develop systems that execute this process with robotic assistance under a variety of widely available and deployable image modalities, including ultrasound, x-ray fluoroscopy, and conventional MRI and CT scanners. Initially, we focus on solid organ therapy, in particular the prostate, but will extend and apply these results to other organ systems, such as the brain, liver, bones and spine. As these results become available, they will be combined with image analysis, data fusion, and reconstruction methods developed in parallel research programs. Typical applications of this enhanced system include vertebroplasty, spine nerve block injections, and bone biopsies, incorporating novel techniques for non-straight-line delivery trajectories.

Recent advances in medical imaging have propelled minimally invasive image-guided percutaneous biopsy and local therapies into public attention [1,2]. Intra-operative radiological imaging has become more accurate, faster, affordable, and less toxic to both patients and surgeons. The objective of the presented work was to meet the ultimate challenge of these procedures and provide seamless integration of intra-operative CT imaging with precise, reliable, and affordable aiming and delivery of percutaneous surgical devices. One could ask why we pursued CT guidance instead of fluoroscopic or ultrasound navigation? Computed tomography (CT) provides good tissue differentiation from even a single slice acquisition and has proven to be an excellent image guidance modality for percutaneous tumor biopsy and drainage [3,4,5] as well as for neurological pain management [6,7,8,9,10]. We also believe that every modality is important and indispensable on its own right. In fact, the system we are presenting lends itself equally well to CT, MRI, Ultrasound, and fluoroscopic navigations. One of the fundamental goals of our percutaneous research program at the Johns Hopkins University is to develop such modular and factorable image-guided robotic surgery systems that, to a large extent, are invariant to the imaging modality with which they are deployed.

2 Clinical Significance

The proposed system has potential use in a wide range of percutaneous interventions. Figure 2 shows the seamless transition from the current phantom setup to applications in abdominal, prostate, and spine procedures. For “flagship application” we selected

CT-guided percutaneous pain management, initially nerve blocks and facet joint injections in the lumbar spine, as well as prostate cancer therapy.

Figure 2: The robotic system used in the phantom experiment is easily deployable in prostate, spine, and abdominal treatments

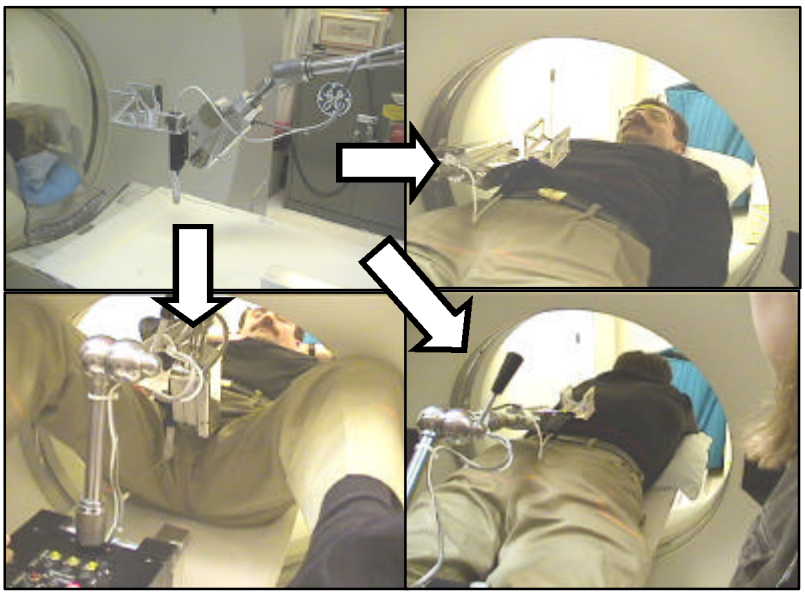

Spinal disorders are undoubtedly the fastest growing musculoskeletal subspecialty, consuming an estimated $120 billion dollars for direct and indirect costs. The acceleration in the number of new cases treated annually reflects the aging of our society as well as the dramatic transformation of the traditional workplace into offices that impose extreme stress on the skeletal system, primarily on the spine. Minimally invasive percutaneous pain management in the spinal region has gained a lot of interest lately. CT-guided nerve blocks and facet joint injections have proven to be safe and effective methods to alleviate severe pain and provide longstanding relief for patients of all age and sex [7,8,9,10]. From a technical point of view, due to the relatively low complexity of the procedure, nerve blocks and facet joint injections are ideally suitable for robotic assistance. Typically, these procedures require a single puncture with a thin needle across reasonably superficial soft tissue, and the use of a single CT image. The workflow of a manual procedure is practically identical to the steps followed by our robotic system. This parallelism offers a unique opportunity for gradual transition from a fully manual procedure to a fully robotic intervention. However simple and easy these procedures may look, there is a great need for precise and consistent aiming and delivery of the needle. The longevity of pain relief is thought to be associated with the spatial accuracy of needle placement. The procedure presents large variability from surgeon to surgeon Longer

times are usually associated with occasional misplacement of the needle, often several times, before its correct position is confirmed. Misplacements also include over-pushing the needle, which causes sharp pain to the patient and must be avoided at all cost. Very importantly, each misplacement of the needle necessitates an extra CT image, each time exposing the patient to unnecessary toxic radiation.

Adenocarcinoma of the prostate is a significant health problem in the Western hemisphere. After cardiac diseases and lung cancer, metastatic prostate cancer is the third leading cause of death among the American man over fifty years of age. Due to the evolving screening techniques, more and more cases are diagnosed at early stage, when the patient can be a candidate for some form of minimally invasive localized therapy, such as radioactive seed implant, and recently gene therapy or some modality of thermal ablation. Contemporary biopsy and intraprostatic delivery of therapeutics are primarily performed under transrectal ultrasound guidance. In many respects, the evolution of localized prostate therapies can be viewed as an evolution of noninvasive visualization. If the implanted needles can be accurately monitored and their placement controlled as they release their payload inside the prostate, then it is theoretically possible to deposit the therapeutic agent (ionizing radiation, heat, cold, genetic agents, etc.), while minimizing unwanted treatment of surrounding normal tissue like the urethra. With the development of spatially accurate real-time 3D hardware and software coupled with accurate robot-augmented placement, this ideal can be achieved. Our approach to the problem was to maintain the largely successful transperineal access, while replacing the manual technique with a robotic needle insertion system, which allows entering needles in arbitrary angle, anywhere over the entire perineum.

3 Prior Engineering Art

Extensive previous work has been done in biopsy and treatment of intracranial lesions using invasive stereotactic head-frames during the last two decades [11,12,13,14,15,16, 17,18]. Early experiences with CT-guided robots were also associated with invasive head-frames [19,20,21].

For procedures that require access to the abdomen or spine, full-body stereotactic frames were developed [22,23,24,25,26]. Devices like Elekta's Stereotactic Body Frame® or MedTEC's BodyFIX® were designed for fractionated stereotactic radiotherapy and never took ground in interventional procedures. These devices typically include some cradle with a mold or vacuum bag that may be difficult to apply for immobile patients. The cradle and fiducials can also interfere with the treatment site,

leaving insufficient room for the intervention inside the gantry. Economically, they were especially unpromising for simple procedures like nerve blocks or facet joint injections.

Handheld manual devices [27,28,29,30] provide valuable help, but do not solve the ultimate problem of the strong coupling between the image space and the surgical device. The efficacy of these predominantly manual approaches depends primarily on the surgeon's hand-eye coordination and ability to interpret visual feedback.

Masamune et al. presented a coach-mounted isocentric needle insertion manipulator that acts inside the CT gantry [31]. This system occupies the surface of the coach and reaches into the field through the far end of the gantry, therefore it is suitable only for intracranial procedures.

Loser proposed a remote center of motion robotic arm manipulated through visual servoing under CT-fluoroscopy [32]. Shortcomings of this approach include the need for CT-fluoroscopy option on the scanner and controlled motion of the CT couch. Neither of these features is widely available, leaving the system unsuitable for most CT scanners.

A few commercial robotic needle insertion systems, such as the Neuromate robot from Integrated Surgical Systems, CA, also exist. Although this robot has been cleared by FDA for stereotactic needle punctures, it does not lend itself well to in-scanner applications due to its relatively large size and heavy built.

Stoianovici et al. developed a compact and dexterous remote center of motion robot conjunctly with a radiolucent needle driver [33]. The system was used for percutaneous access to the kidney under joystick control with C-arm fluoroscope. This system has proven to be an excellent percutaneous robotic aid, but did not provide computerized remote control, which is necessary for computer-aided path planning and execution. Patriciu et al. have used the laser light of the CT scanner to register the same robot to the CT scanner and achieved in-CT needle puncture [35].

Susil et al. [34] proposed a small version of the Brown-Robert-Wells (BRW) head-frame for single slice based registration of manipulators to image space inside a CT scanner and provided valuable robustness and sensitivity analysis of the image registration method.

4 Our Approach

The presented system combines the favorable features of Stoianovici's Susil's work in a prototype of a percutaneous CAD/CAM system.

Manual needle punctures typically include the following three decoupled tasks: (1) touch down with the needle tip on the skin entry point, (2) orient the needle by pivoting around the skin entry point, (3) insert the needle to the body along a straight trajectory. Inserting a needle to an arbitrary location requires six independent stages of motion, also called degrees-of-freedom or DOF. First, three independent Cartesian motions (3-DOF) are necessary to move the needle tip from its current location to the skin entry point. Then two independent rotations (2-DOF) are necessary to aim the needle by pivoting around a fulcrum point at the skin entry point. Finally, one-directional translation (1-DOF) is necessary to insert the needle into the body through the skin. This kinematic sequence can be achieved by the basic robotic system shown in Figure 3.

Figure 3: Basic robotic components assembled for percutaneous needle insertion (Important note: Before using the system, the tip of the needle must be positioned at the fulcrum point of the rotational stage. In the picture below the needle and its guide have not been adjusted to the center of motion.)

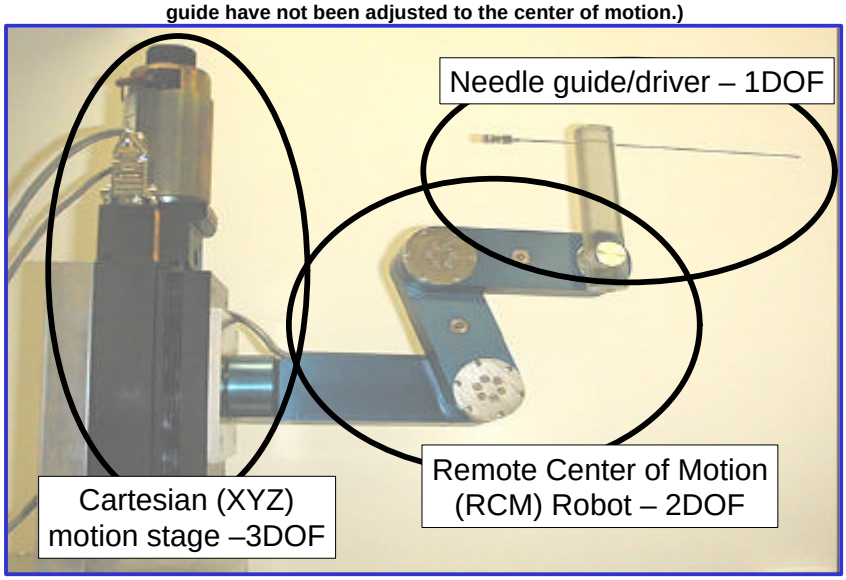

The robotic components have been developed by primarily Stoianovici, Taylor, and Whitcomb at the Johns Hopkins University [33,35,36,37]. The system consists of a 3-DOF Cartesian motion stage, a 2-DOF rotational stage, and a 1-DOF needle insertion stage. The stages are operated sequentially. Only one stage is moving at a time while motion power is turned off on the two other inactive stages. This scheme prevents insertion before proper alignment is confirmed and also prevents accidental changing of the needle path during insertion The stages are kinematically constrained and each stage is able to perform only one kind of motion. For example, the rotation stage cannot translate and the translational stage cannot rotate. The system also applies non-backdrivable transmission that preserves configuration when the robot is deactivated

or in the event of power failure. Over-travel of the stages is also a concern that is addressed extensively in the control software and by placing hard-stop blocks on the hardware. For example, accidental over-travel of the needle can be prevented by placing a sterile clamp on the needle shaft above the driving gear at the maximum insertion depth. These safety features guarantee that the robotic system performs only the prescribed

Figure 4: Schematic drawing of the prototype system

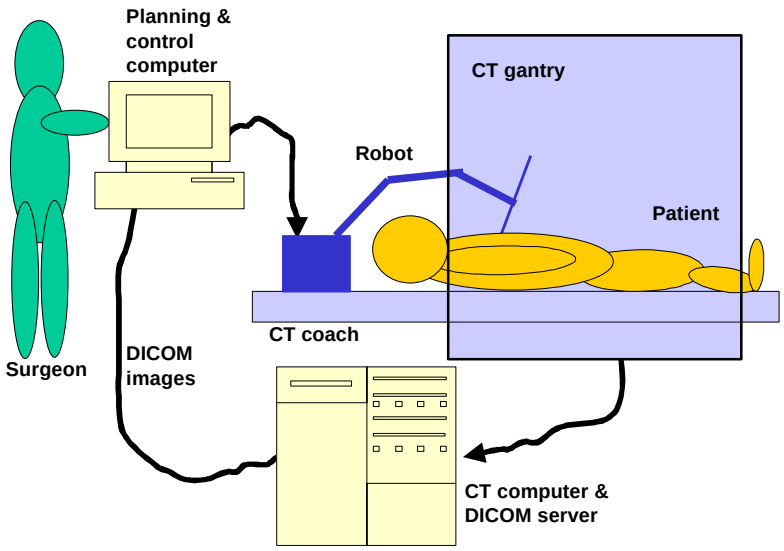

motion and each component stays within the set kinematic constraints. These robotic components have been used in multiple clinical scenarios at the Department of Urology of the Johns Hopkins University and their engineering characteristics have been published extensively [35,36,37].

A schematic drawing of the overall configuration of the prototype system is presented in Figure 4. The CT images are transferred across a local area network (LAN) in DICOM format to a Pentium-II 333 MHz personal computer equipped with a 17" flat panel display. The computer runs a "simple storage" DICOM server, installed from the public domain source at http://www.erl.wustl.edu/DICOM [38]. The operator of the scanner pushes DICOM images from the CT console through the LAN to the DICOM server. The central computer provides intra-operative image processing, motion planning, remote actuation, and control of the robotic components. These services are provided by the 3D Slicer, which is jointly developed with MIT Artificial Intelligence Laboratory and the Surgical Planning Laboratory at the Brigham and Women Hospital [39]. Figure 5 shows screenshots from the 3D Slicer-based path planning and visualization system. The

surgeon uses an interactive display to execute the intervention step-by-step. Upon completing each step, the computer waits for confirmation before continuing. The interactive software completes an intra-operative control loop, thus implementing a simplified variant of the surgical CAD/CAM paradigm. The central computer enables the gathering of complex intra-operative information. Post-operational processing of these data is expected to become valuable for outcome analysis, rehabilitation planning, as well as for the performance evaluation of the engineered system.

Figure 5: Path planning in the 3D Slicer system

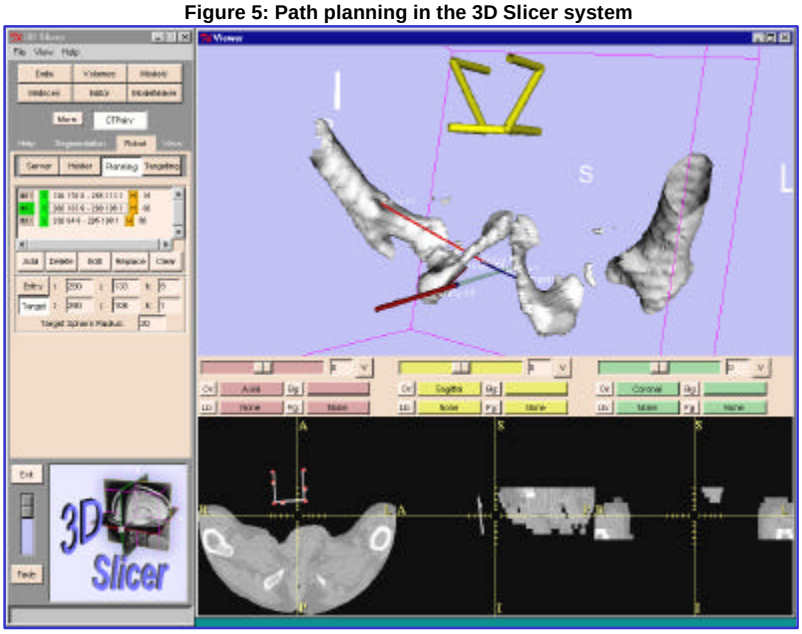

The actual pre-clinical prototype is shown in Figure 6. Here the robotic system is mounted on the CT coach. In order to promote encapsulation of robotic components, the amplifiers and power supplies are built inside the robot mount. Temporarily, the Cartesian motion stage was replaced by an un-encoded passive mounting arm. The arm locks and unlocks easily with a handle. We unlock arm, move the robot manually to the skin entry point, then we lock the arm. The rotational stage is attached to the arm, then the radiolucent motorized needle insertion device (needle driver) is attached to the rotational stage. The needle driver is an invention of Stoianovici et. al [33].

The system applies purely image-based registration between the robot and the image space by mounting a stereotactic frame permanently on the robot's end-effector. The device does need calibration and performs and registration and targeting on a single image slice, thus promoting lower radiation exposure and a shorter procedure.

The system does not depend on any vendor-specific hardware or software feature and is deployable on any scanner that has DICOM interface. The combined weight of the

Figure 6: Pre-clinical prototype system

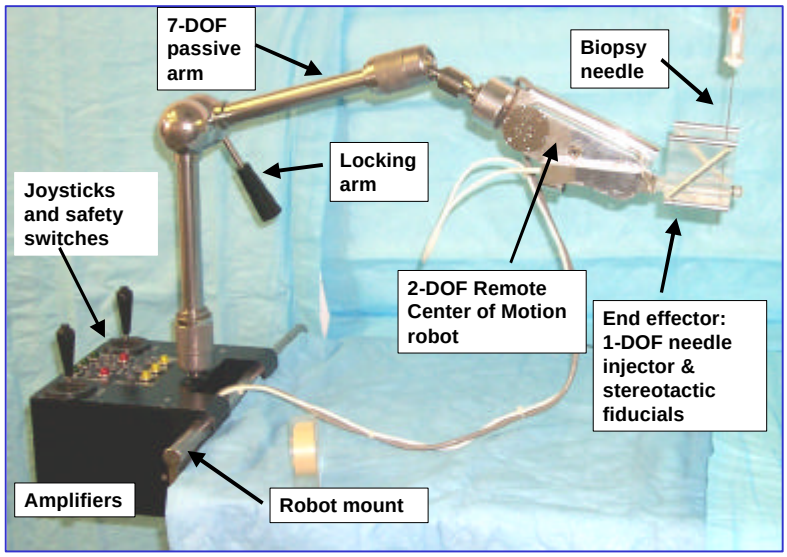

system is about 15 kg. One reasonably skilled technician can set up and take down the system in ten minutes. The passive arm, RCM robot, and needle driver fold conveniently into a carry-on suitcase.

5 Novel End-Effector

Like in any image-guided surgical system, accurate and robust registration between the surgical instrument and the image space is crucial. In order to achieve fully image-based registration, rigid body fiducials were applied. As we discussed earlier, invasively attached head-frames and body-frames did not fare well in procedures performed inside a CT gantry. Susil's [34] method (attaching a rigid body fiducial pattern to the end-effector) seemed to be a viable solution. Because CT images are taken in transverse direction with potential gaps between them, a fiducial pattern combined from straight rods is the most obvious choice. These fiducials system, like the BRW or Leksell frames, have been used in similar circumstances for decades, and their accuracies and error characteristics are well documented [15,16,17,18]. Susil et al. in [34] also proved that the Z-shape fiducial motifs of the conventional stereotactic head-frames demonstrate

favorable error characteristics, accuracy, and reliability in a large angular range. In our design (Figure 6), the combined needle driver and fiducial system form a rigid body of known dimensions. In the miniaturized frame, two adjacent Z-shape motifs share a common fiducial rod, thus there are only seven marks in each CT slice instead of the conventional nine marks. This design feature, however, has no effect on the essence and accuracy of the registration.

The needle injector employs the kinematic principle "Friction Transmission with Axial Loading," invented by Stoianovici [33]. The transmission is uniquely suited for a miniaturized radio-lucent construction to provide motorized needle actuation. A unique feature of this device is that it grasps the barrel of the needle instead of its head. This solution significantly reduces the unsupported length of the needle, which, in turn, reduces lateral flexure during injection and increases the accuracy of insertion.

The main parts of the needle driver are made of acrylic, which provides sufficient rigidity while producing negligible artifacts in CT images. The Z-shape markers are assembled from seven cylinders of 5 mm diameter. The cylinders are filled with X-ray blocking liquid (HYPAQUE: Nyromed Inc., NJ, U.S.A., at 65% concentration), so the cylinders produce solid marks in CT. The size of the bounding box defined by the central axes of the fiducial rods is 60x60x60 mm^3.

Friction driving does not allow for predictable depth control due to occasional slippage. Should the transmission slip, the needle stops short and is guaranteed not to overshoot the target. For further safety, we can fix a sterilized spring loaded clamp on the needle at the intended insertion depth. This fixture indicates whether the needle has slipped and stopped shallow and, very importantly, provides an extra safety measure against over-driving the needle. Should the needle stop short due to transmission slippage, we can drive the needle to the correct depth under direct joystick control, using the needle clamp as a depth indicator.

6 Registration and Targeting

In our approach, one CT slice is necessary and sufficient for the calculation of needle orientation and insertion depth, assuming that the target and all fiducial rods are visible in the image. Our registration method produces a closed form solution and there is no need for initial posture estimation or guess. The method is reliable in a wide range of rotations, as Susil reported previously in [34]. The skin entry point, which is identical to the remote

center of motion remains constant with respect to the stereotactic frame. Because the fulcrum point of the robot remains constant for the entire lifetime of the robot and end-effector, the system never needs calibration. Targeting with the robotic device takes place in the following steps:

1. Identify the marks of the fiducials and target point in the CT image.
2. Ascertain the pixel size of the CT image. (We also assume that the images are sufficiently free of distortion, which is true for most current scanners. Therefore, the registration does not require calibration of the CT scanner.)
3. Calculate the six DOF transformation matrix that will take the target point from image coordinates to stereotactic frame coordinates.

The geometric description of all three Z-shape motifs, as well as the spatial relation among the three Z-shape motifs, are a priori known. When an image plane intersects with a Z-shape motif, the three rods produce three distinctive marks in the image. In our miniaturized frame, two neighboring Z-shape motifs share a fiducial rod, so there are only seven marks in each CT slice, as shown in Figure 7.

Figure 7: Fiducial marks of the stereotactic registration device in a CT image. (The image was taken with the prostate implant training phantom.)

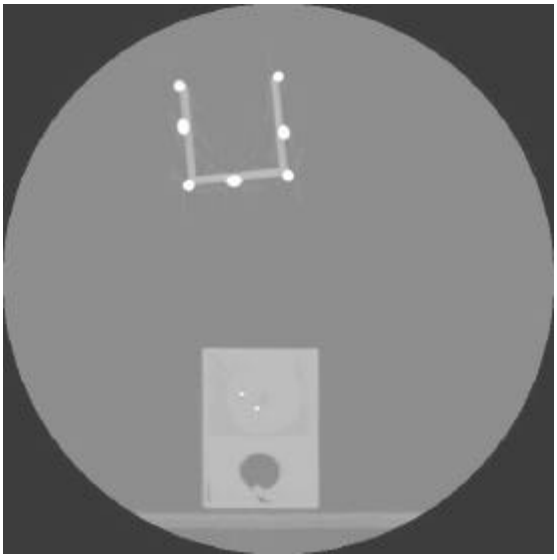

We use standard image processing steps to obtain the positions of the seven markers in image pixel coordinates. In the registration, we calculate the position of the mark on the slanted rod in each Z-shape motifs, then we obtain their locations with respect to the fiducial frame. The three intersection points with the three slanted rods are guaranteed not to be collinear and they are always sufficiently distant from each other and never

produce a deformed triangle. From here, the process of deriving the Image→Frame transformation matrix is reduced to a rigid body registration problem between two triangles. We look for the 6-DOF transformation matrix, which takes the rigid triangle from image coordinates to stereotactic frame coordinates. Once the Image→Frame transformation is available, the targeting algorithm proceeds as summarized below.

1. Apply the Image→Frame transformation to the target point and obtain the target in the coordinate space of the stereotactic frame.
2. Calculate the 2 DOF rotation matrix that will be applied to rotate the needle around its tip, so that the needle is aligned with the target. First we calculate the straight line that connects the (already transformed) target point and the remote center of motion. This line represents the desired orientation of the needle. Then, we calculate the two rotations that take the needle from its current orientation to its desired orientation.
3. Calculate the insertion depth, which is available as the distance from the target point to the remote center of motion (i.e. the tip of the needle).

7 Experiments

We have performed three series of phantom experiments with the presented system using GE Signa CT scanner at the Division of Interventional Neurology of the Johns Hopkins University. Standard 17G diamond-head needles were used and 2 mm implanted steel balls served as targets throughout the experiments (Figure 8).

Figure 8: Phantom experiments with honeydew melon, prostate implant training phantom, and anthropomorphic phantom

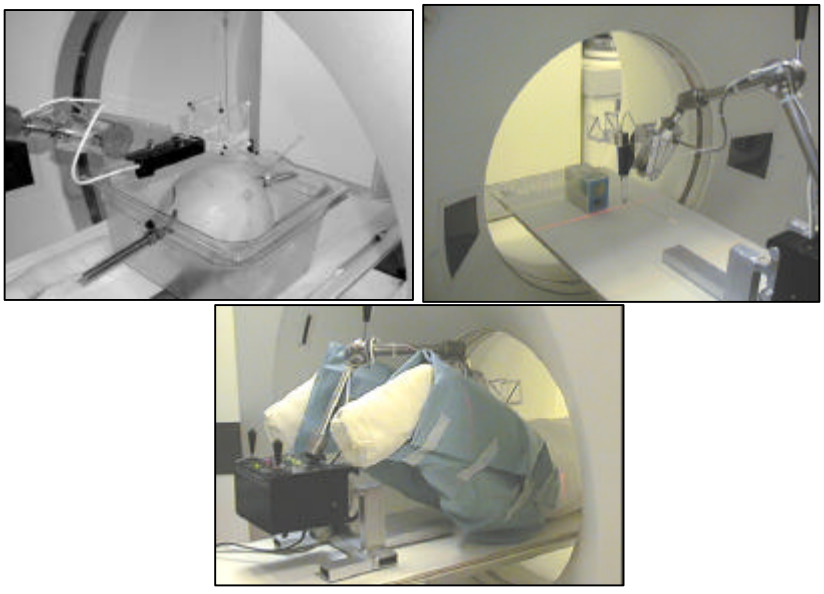

In the first series a honeydew melon represented the patient In the second series a standard off-the-shelf prostate implant training phantom (Nuclear Associates, NY) was applied In the third series, actual clinical circumstances were simulated on an anthropomorphic phantom. A full body plaster cast of a volunteer (one of the authors) was produced, then a life-size torso with moveable joints was assembled from the cast. Finally, a prostate training phantom (Nuclear Associates, NY) was inserted into the torso, in a way that the overall size and the lay-out of organs reasonably represented an average male body.)

8 Results and Discussion

In open air, where there is no needle-tissue interaction, we systematically achieved an accuracy better than 1 mm, in hitting targets at 5-8 cm from the fulcrum point.

Confirmation images from melon experiment is shown in Figure 9. In the transverse image (right), the tip of the needle accurately hits the target. In the corresponding projected scout view (left) a slight bending of the needle can also be observed. The orientation accuracy was determined to be 0.6°, and the distance between the needle tip and the target was 1.04 mm. Consistent results were achieved in the ultrasound training and full-body phantoms.

Figure 9: Confirmation images after needle insertion into the honeydew phantom . Scout view with target, needle, and robot (L). Image slice with implanted target, needle tip and end-effector frame (R).

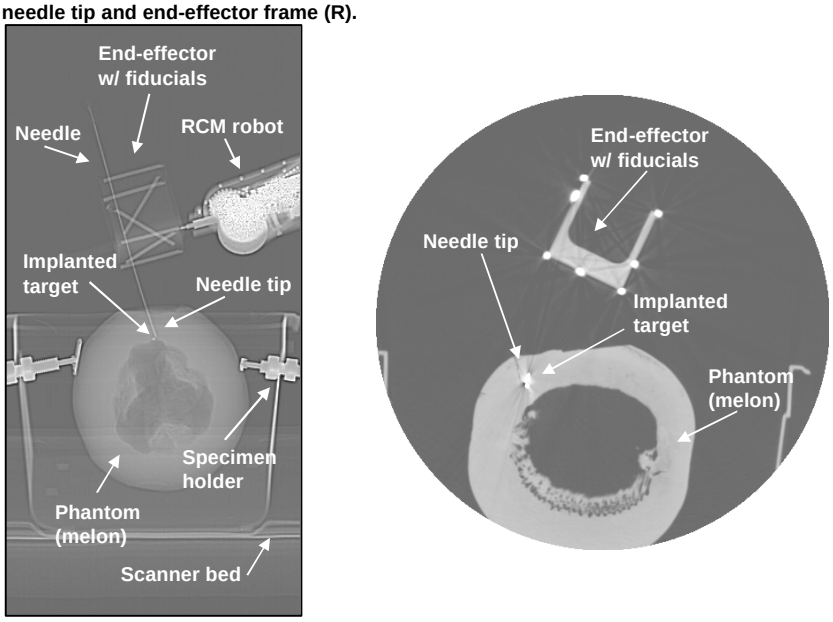

Our experiments suggest that the primary cause of needle placement error is needle-tissue interaction. Inhomogeneities in the penetrated body tissues may cause substantial needle placement error. Ideally, the needle should be perpendicular to the skin surface in order to avoid slippage and deflection of the needle. Detailed analysis of these effects must be studied in further experiments.

Our current needle driver uses friction transmission which is associated with a maximum exertion force. If the resistance of the tissue is greater than the maximum transmission force, then the needle will slip and stop short of the target. We experienced occasional slippage of the needle in the phantom experiments. Worse yet, multiple insertions increase the likelihood of slippage, because fluids can get into the transmission mechanism during the retraction of the needle. In order to reduce the possibility of slippage, we made small incision on the surface of the phantom under the needle tip. However, incision is not a viable clinical option when multiple needles are delivered in a complex pattern. The current needle driver also cannot release its grasp on the needle while the needle is inside the body, which may be a problem if involuntary movement of the patient can be anticipated. In an answer to these problems, a novel needle driver with frictionless transmission and needle-release option has been already developed.

Replacing the passive arm with an active 3 DOF Cartesian motion stage is a work in progress. The skin entry point will be picked from the CT images, and the Cartesian stage will move the needle to the entry point. This feature is required for delivering multiple needles in a complex pattern.

Clinical safety is a crucial issue, which, unfortunately, could be addressed only tangentially in this article. In general, clinical trial on human subjects cannot be planned without a detailed safety evaluation of the entire system, including the robot, the end-effector, and the control software. This is a major work in progress.

9 Conclusion

We have demonstrated the technical feasibility of robotically assisted needle insertion inside a CT scanner, both in and perpendicular to the transverse image plane. Experiments with mechanical phantoms indicated that this robotic system may be suitable for various percutaneous clinical applications. Compared to other known robotic systems, our system appears to be smaller, simpler, easier to use, and more cost-effective. Further experiments are needed to evaluate the accuracy and safety of the system before applying it on human subjects.

10 Acknowledgments

The authors acknowledge the support of the National Science Foundation under the Engineering Research Center grant #EEC9731478 and the Japanese government under the grant #JSPS-RFTF99I00904. Our work was also co-sponsored by AdMeTech, the Henry M. Jackson Foundation, and the US Army Medical Research and Material Command, as well as by the Whiting School of Engineering of the Johns Hopkins University. We gratefully acknowledge the long standing support of Dr. Louis R. Kavoussi at the Brady Urological Institute. We are also obliged to Drs. David M. Yousem and Kieran Murphy for housing the experiments at the Division of Interventional Neurology. Last but not least, we are indebt to Vincent L. Lerie, R.T for spending many long hours with us in the scanner room, and without whom our research would not have been as much fun as it was.

11 References

[1] Jain RK (1997) The next frontier of molecular medicine: Delivery of therapeutics. Nature Medicine 4:655-657.

[2] Klausner RD (1997) The Nation's Investment in Cancer Research: A Budget Proposal for Fiscal Year 1999. National Cancer Institute.

[3] Yousem DM, Sack MJ, Scanlan KA. (1994) Biopsy of parapharyngeal space lesions. Radiology 1994; 193: 619-622.

[4] Yousem DM, Sack MJ, Weinstein GS, Hayden RE. (1995) Computed tomography- guided aspirations of parapharyngeal and skull base masses. Skull Base Surgery 1995: 5: 131-136.

[5] Sack MJ. Weber RS. Weinstein GS. Chalian AA. Nisenbaum HL. Yousem DM. (1998) Image-guided fine-needle aspiration of the head and neck: five years' experience. Archives of Otolaryngology -- Head & Neck Surgery. 1998, 124(10):1155-61.

[6] Jacob AL; Messmer P; Kaim A; Suhm N; Regazzoni P; Baumann B (2000) A whole-body registration-free navigation system for image-guided surgery and interventional radiology. Invest Radiol 2000 May;35(5):279-88

[7] McDonald JS (2000) Computer driven needle probe enables therapy for painful neuropathies. Stud Health Technol Inform 2000;70:202-6

[8] Gangi A; Dietemann JL; Mortazavi R; Pfleger D; Kauff C; Roy C (1998), CT-guided interventional procedures for pain management in the lumbosacral spine.. Radiographics 1998 May-Jun;18(3):621-33

[9] Pelz DM; Haddad RG (1989), Radiologic investigation of low back pain. CMAJ 1989 Feb 1;140(3):289-95

[10] Proske M; Steinbrich W (1996), CT-guided pain treatment, Schweiz Med Wochenschr 1996 Jul 20;126(29):1270-3

[11] Brown, R. A. (1979), A stereotactic head-frame for use with CT body scanner. Invest. Radiol., 1979. Vol. 14: pp 300-304.

[12] Brown R. A., Roberts T. S., and Osborne A. G. (1980) Stsreotactic frame and computer software for CT-directed neurosurgical localization. Invest. Radiol., 1980. Vol. 15: pp 308-312.

[13] Goers S., et al. (1982) A computed tomographic stereotactic adaptation system. Neurosurgery, 1982. Vol. 10, pp 375-379.

[14] Leksell L. and Jerenberg B. (1980) Stereotaxis and tomography: a technical note. Acta Neurochir., 1980, Vol. 52, pp 1-7.

[15] Galloway RL Jr; Maciunas RJ; Latimer JW (1991) The accuracies of four stereotactic frame systems: an independent assessment. Biomed. Instrum. Technol. 1991 Nov-Dec; 25(6):457-60

[16] Maciunas RJ; Galloway RL Jr; Latimer J; Cobb C; Zaccharias E; Moore A; Mandava VR (1992) An independent application accuracy evaluation of stereotactic frame systems. Stereotact. Funct. Neurosurg. 1992;58(1-4):103-7

[17] Maciunas RJ; Galloway RL Jr; Latimer JW (1994) The application accuracy of stereotactic frames. Neurosurgery 1994 Oct;35(4):682-94; discussion 694-5.

[18] Zylka W, Sabczynski J, Schmitz G (1999) A Gaussian approach for the calculation of the accuracy of stereotactic frame systems. Medical Physics, 26: (3) 381-391 MAR 1999

[19] R.F. Young (1999) Application of robotics to stereotactic neurosurgery, Neurological Research, vol. 9., pp. 123-128, 1987

[20] Y.S. Kwoh, J. Hou, E.A. Jonckeere, S.Hayati (1988) A robot with improved absolute positioning accuracy for CT guided stereotactic brain surgery, IEEE Transactions on Biomedical Engineering, 35(2), pp. 153-160, 1988

[21] J.M. Darke, M. Joy, A. Goldenberg, et. al. (1991) Computer and robotic assisted resection of brain tumors, Proc. 5th Intern. Conference on Advanced Robotics, pp. 888-892, 1991

[22] Lax I, et al. (1994) Stereotactic radiotherapy of malignancies in the abdomen. Methodological aspects. Acta Oncol. 1994;33(6):677-83.

[23] Erdi Y., Wessels B., DeJager R., Erdi A., et al. (1994) A new fiducial alignment system to overlay abdominal CT or MR images with radiolabeled antibody SPECT scans, Cancer, 1994;73 (3 Suppl):923-931.

[24] Henric Blomgren, Ingmar Lax, Hakan Goranson, Thomas Kraepelien et al (1998). Radiosurgery for Tumors in the body: Clinical experience using a new method. Journal of Radiosurgery Vol.1. No.1: 63-75.

[25] Takacs I, Hamilton AJ (1999) Extracranial stereotactic radiosurgery: applications for the spine and beyond. Neurosurg Clin N Am 1999 Apr;10(2):257-70.

[26] Lohr F, et al (1990) Noninvasive patient fixation for extracranial stereotactic radiotherapy. Int J Radiat Oncol Biol Phys 1999 Sep 1; 45(2): 521-7.

[27] A.M. Pelastrant (1990) Comprehensive approach to TC-guided procedures with a hand-held device, Radiology, vol. 174, pp. 270-272, 1990

[28] H. Ishizaka, T.Katsuya, Y. Koyama, H. Ishijima, T. Moteki, et al. (1998) CT-guided percutaneous intervention using a simple laser director device, AJR, 170(3), pp.745-746, 1998

[29] A. Gangi, B.Kastler, J.M.Arhan, A. Klinkert, et al. (1994) A compact laser beam guidance system for interventional CT, J. of Comp. Assisted Tomography, 18, pp. 326-328, 1994

[30] C. Frahm, W. Kloeess, H.B.Gehl, et al. (1004) First experiments with a new laser-guidance device for MR- and CT-guided punctures, European Radiology, vol. 5, p 315, 1994

[31] Masamune, K., Ji, L-H., Suzuki, M., Dohi, T., Iseki, H., Takakura, K. (1998) A Newly Developed Stereotactic Robot with Detachable Drive for Neurosurgery, Lecture Notes in Computer Science, Proc. of MICCAI98, Boston, pp. 215-222. , Springer-Verlag.

[32] M. Loser, N. Navab (2000) A new robotic system for visually controlled percutaneous interventions under CT. Proceedings to *Medical Image Computing and Computer-Assisted Intervention*, 2000; Lecture notes in computer science, Vol 1935, pp 887-897, Springer Verlag, 2000.

[33] Stoianovici, D., Cadeddu, J. A., Demaree, R. D., Basile, H. A., Taylor, R. H., Whitcomb, L. L., Sharpe, W. N. Jr., Kavoussi, L. R. (1997) An Efficient Needle Injection Technique and Radiological Guidance Method for Percutaneous Procedures, Lecture Notes in Computer Science, 1997 CVRMed-MRCAS, Springer-Verlag, Vol. 1205, pp. 295-298.

[34] Susil, R. C., Anderson, J. H., Taylor, R. H.,(1999) A Single Image Registration Method for CT-Guided Interventions. Lecture Notes in Computer Science, MICCAI99, Springer-Verlag, Vol. 1679, pp. 798-808.

[35] Alexandru Patriciu, Stephen Solomon MD, Louis Kavoussi MD, Dan Stoianovici PhD, "Robotic Kidney and Spine Percutaneous Procedures Using a New Laser-Based CT Registration Method". *Fourth International Conference on Medical Image Computing and Computer-Assisted Intervention (MICCAI)*, Utrecht, The Netherlands 14-17 October 2001. (accepted for publication.)

[36] Cadeddu, J.A., Stoianovici, D., Chen, R.N., Moore, R.G., Kavoussi, L.R., (1998), Stereotactic mechanical percutaneous renal access, *Journal of Endourology*, Vol. 12, No. 2, April 1998, p. 121-126.

[37] Cadeddu, J.A., Stoianovici, D., Chen, R.N., Moore, R.G., Kavoussi, L.R., (1998)

Mechanical percutaneous renal access, *Journal of Urology*, Vol. 159, No. 5, p.110. (1998)

[38] Russell Taylor, Patrick Jensen, Louis Whitcomb, Aaron Barnes, Rajesh Kumar, Dan Stoianovici, Puneet Gupta, ZhengXian Wang, Eugene deJuan, and Louis Kavoussi, (1999) A Steady-Hand Robotic System for Microsurgical Augmentation. International Journal of Robotics Research, (18)12, December 1999.

[39] DICOM Web Home Page; http://www.erl.wustl.edu/DICOM/

[40] D. Gering, A. Nabavi, R. Kikinis, W. Eric L. Grimson, N. Hata, P. Everett, F. Jolesz, W. Wells III. An Integrated Visualization System for Surgical Planning and Guidance using Image Fusion and Interventional Imaging. Medical Image Computing and Computer-Assisted Intervention (MICCAI), Cambridge England. Lecture Notes in Computer Science, MICCAI99, Springer-Verlag, Vol. 1679, pp. 809-819

[41] Schorr O, Hata N, Bzostek A, Kumar R, Burghart C, Taylor RH, Kikinis R, Distributed Modular Computer-Integrated Surgical Robotic Systems: Architecture for Intelligent Object, Medical Image Computing and Computer-assisted Intervention 2000, Pittsburgh, PA Lecture Notes in Computer Science, MICCAI 2000, Springer-Verlag, Vol. 1935, pp. 969-987